Darcy Forchheimer nanofluid thin film flow of SWCNTs and heat transfer analysis over an unsteady stretching sheet

Cite as: AIP Advances **9**, 015223 (2019); https://doi.org/10.1063/1.5083972
Submitted: 02 December 2018 • Accepted: 11 January 2019 • Published Online: 23 January 2019

Saleem Nasir, Zahir Shah, Saeed Islam, et al.

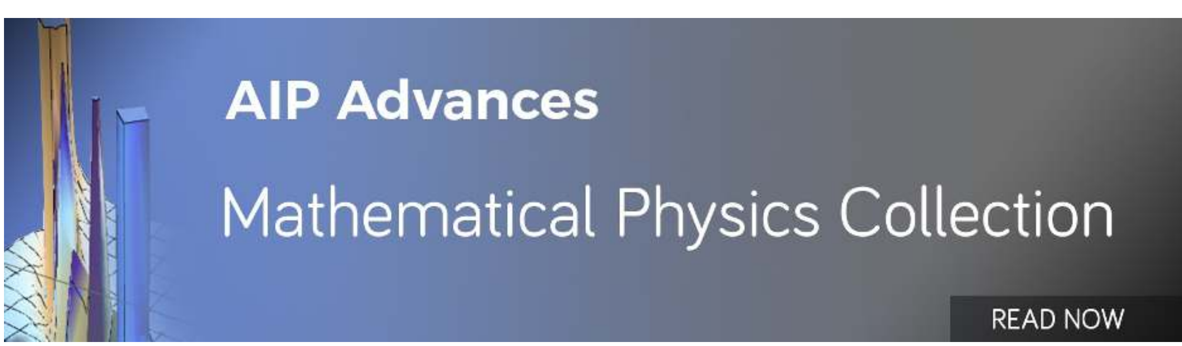

Darcy Forchheimer nanofluid thin film flow of SWCNTs and heat transfer analysis over an unsteady stretching sheet

Cite as: AIP Advances 9, 015223 (2019); doi: 10.1063/1.5083972
Submitted: 2 December 2018 • Accepted: 11 January 2019 •
Published Online: 23 January 2019

Saleem Nasir,[1,a] Zahir Shah,[1,a] Saeed Islam,[1,a] Ebenezer Bonyah,[2,b] and Taza Gul[3,c]

AFFILIATIONS

[1] Department of Mathematics, Abdul Wali Khan University, Mardan, 23200 Khyber Pakhtunkhwa, Pakistan
[2] Department of Mathematics Education, University of Education Winneba Kumasi -(Kumasi Campus), 00233, Ghana
[3] Departement of Mathematics, City University of Science and Information Technology, Peshawar, Khyber Pakhtunkhwa 25000, Pakistan

[a] saleemnasir85@gmail.com; zahir1987@yahoo.com; saeedislam@awkum.edu.pk
[b] **Correspondence:** ebbonya@gmail.com
[c] tazagul@cusit.edu.pk

ABSTRACT

This article analyzes the Darcy Forchheimer 2D thin film fluid of nanoliquid. Flow of nanoliquid is made due to a flat unsteady stretchable sheet. In nanoliquids, nanomaterial is in form of CNTs (carbon nanotubes). Also, in present analysis, single walled carbon nanotubes (SWCNTs) are accounted as nanoparticles. The classical liquid 'water' is treated as based liquid. The flow in permeable region is characterized by Darcy–Forchheimer relation. Heat transport phenomena are studied from convective point of view. The transformation of partial differential set of equations into strong ordinary differential frame is formed through appropriate variables. Homotopy Analysis Method (HAM) scheme is executed for solving the simplified set of equations. In addition, a numerical analysis (ND-Solve) is utilized for the convergence of the applied technique. The influence of some flow model quantities like P_r (Prandtl number), λ (unsteadiness factor), k (porous medium factor), F (Darcy-porous medium factor) on liquid velocity and thermal field are scrutinized and studied through sketches. Certain physical factors like $f''(0)$ (friction factor coefficient) and $-\theta'(0)$ (rate of heat transport) are first derived and then presented through tables.

I. INTRODUCTION

In recent time, the transformation of heat developing nano-fluids is among the hot field of analysis due to their encouraging heat transfer characteristics while equated with classical heat transfer liquids like kerosene oil, gasoline oil, water, ethylene glycol and many other.[1,2] Nanoliquids are considered as the finest coolants in numerous engineering industries in heat exchange equipment such as transportation, biomedical, micro-electronics cooling systems, optical, solid state illumination and manufacturing etc.[3] Nanoliquids have greater rates of heat transport, high viscosity, superior thermal conductivities and extra stability than other liquids. Nanofluids retain a superior dispersal wetting, and scattering properties on a solid medium. Nanofluids have extraordinary optical features and owing to such features, nanoliquids are used in mechanism of solar collectors. The accessible studies on heat transport of nanofluids are mostly impressive on the development of useful coolants. These coolants can be operated in a widespread heat variety with the enriched thermal conductivities and dropped viscosity. Gireesha et al.[4–6] investigated the convective flow of kerosene-alumina, Maxwell and Jeffrey nanoliquid through exponential space. Also, Gireesha et al.[5] deliberated the impact of heat exchange in the movement of nanoliquid on an upright plate. Sufficient of investigational and theoretic research[6–9] related to the issue of nanoliquids flow has been conferred in research after the effort by Choi and Eastman.[10]

In 1992 Iijima[11] originated carbon nanotubes (CNTs). Carbon nanotubes consist of coiled graphene sheets like a tube configuration of diameter range from 0.7nm to 50 nm. Carbon nanotubes can be subdivided into two main categories, i.e. single-Walled (SWCNTs) and multi-walled (MWCNTs) carbon nanotubes. Furthermore, CNTs (Carbon nanotubes) are predicted inventive matter of 21[lst] century due to their remarkable significance in the field of nanotechnology, hard water, conductive plastics, air refinement scheme, mechanical compound materials, superfluous strong filaments, sensors devices, displays of flat-panel, storage of gas, bio-sensors and many more. Also due to carbon chains in carbon nanotubes do not have any risk to environment. So, it is very important to analyze various properties of CNTs (carbon nanotubes) on the fluid movement and heat transport of liquids. Xue[12] examined the model of thermal conductivities for CNT base mixtures. Ding et al.[13] analyzed some thermal characteristics of CNTs based nanoliquids. Also Imtiaz et al.[14] presented several features of CNTs based nanoliquid flow a stretching surface. Hayat et al.[15] investigated the features of CNTs in an extending flow problem of Darcy-Forchheimer, melting heat and chemical reaction. Mahanthesh et al.[16] discussed the MHD nanoliquid flow containing CNTs nanoparticles with Marangoni convection and thermal radiation impact. Nasir et al.[17] studied the three dimension MHD flow of SWCNTs nanoliquid through stretching sheet.

The significance of finite liquid films can be perceived in a different fields starting from environment to engineering like films of tear in humans eye, the usage of membrane in bio-physics, coating streams and many other industrial trends. The universal existence and useful applications of finite liquid film in nature forced scholars and engineers to study appliance present in such flow of thin film. The utility in the study of lubrication concept, Reynolds[18] presented the dynamics and significance thin film flow model. Oron et al.[19] discussed a joined scientific philosophy for the thin liquid films and discussed a comprehensive analysis on the result stability. Thiele et al.[20] discussed the study the thin liquid flow on an inclined porous surface. Siddiqui et al.[21] examined the flow velocity and surface tension of Sisko finite liquid film through a flat plate. Prashant et al.[22] scrutinized formulation of MHD thin liquid film flow and heat transport through an unsteady extending plate. Similarly, Khan et al.[23] inspected the flow of second grade thin liquid film through a stretchable plate with MHD and thermal radiation impact. Furthermore, recently some relevant and prominent comprehensive survey may be found in Refs. 24–29.

So, in numerous manufacturing system, the liquid flows through an extending surface having remarkable usages, for instance, the warm rolling, melt spinning, extrusion, the wire drawing, production of crystal fiber, plastic and rubber sheets manufacturing etc. Crane[30] formulated the 2D flow over a extending sheet. Also, Wang[31] continued to improve the concept of Crane work to 3D problems. Gireesha et al.[32,33] deliberated the effect of nanoparticles on the flow of nanoliquid through stretching sheet. Also, few more detail suitable new studies about stretching surfaces have been described in the Refs. 34–36.

The liquid flow through a porous surface agrees numerous usages in field of mechanical technology such as the progressions geothermal supplies of water, misappropriation of scattering matter underground, improvement of oil production, combustors of coal, and growth of warmness pipeline and many more. The improved structure of usual (traditional) Darcy theory is non-Darcian porous surface which includes the characteristics of boundary and inertia.

Forchheimer[37] presented an additional relation in momentum which investigates all the characteristics. Muskat[38] called this additional expression Forchheimer relation. But Cheng et al.[39] explored early study on Darcian free convective flow through a uniform upright surface. Later, Merkin40 suggested a suitable similarity alteration for Darcian free convection, but the generalized form of Merkin work was explored by Nakayama et al.[41] Seddeek[42] examined various properties of Darcy-Forchheimer flow. Further some detail latest exploration on Darcy-Forchheimer stream can be attempt by various scholars in Refs. 43–48.

Inspired by the exceeding investigation, in present work, we examined the Darcy Forchheimer two dimensional thin liquid flow of nanoliquid over a stretchable flat sheet. In present analysis single walled carbon nanotubes (SWCNTs) is accounted as nano-materials and water is used as a based liquid. The non-linear system of differential equations is achieved by means of employing appropriate parameter. Technique of HAM[49–55] is method for the solutions. The contribution of various model factors comprising velocity, thermal field is discussed and displayed. The secondary factors of flow, Skin-friction coefficient and heat transfer rate are also investigated graphically.

II. FORMULATION

In this exploration, it is presumed that Darcy Forchheimer 2D single walled carbon nanotubes nano-fluids film is flowing over a flat stretchable sheet. In this work the classical liquid water is treated as based liquid. Furthermore, the upper free surface of the liquid film, which is in interaction with a passive gas, is supposed flat and the influence of surface tension is negligible. The nanoliquid is supposed to be incompressible and the flow is laminar. Also assumed the based liquid (water) and SWCNTs nanoparticles are in thermal equilibrium. The physical problem of thin film flow related concept and coordinates is shown in Figure 1. We consider the surface of sheet at ($y = 0$) stretched then the velocity field at the surface of sheet is[36]

$$U_w = \frac{b}{1-\alpha t}x, \tag{1}$$

Finally, the thermal profile on the sheet is calculated as in the following form[36]

$$T_s = T_0 - T_r\left(\frac{bx^2}{2\nu_f}\right)(1-\alpha t)^{-\frac{3}{2}}. \tag{2}$$

Where α and b are positive factors. (T_r, T_0) the reference and slit temperature, ν_f kinematic viscosity of based fluid.

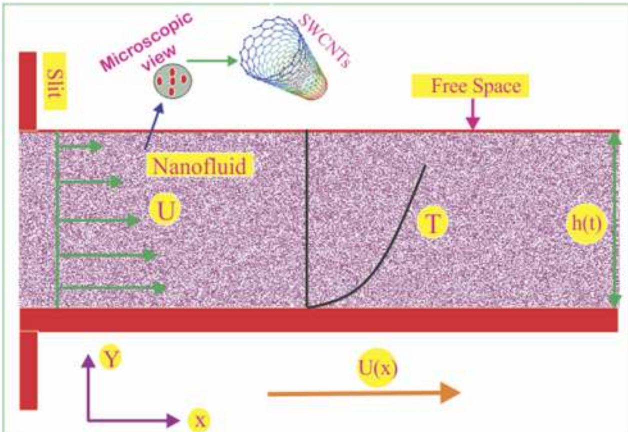

FIG. 1. The schematic diagram of the physical flow model.

In current analysis, we supposed that the gravitational impact is trivial while the liquid film is constant and stable. Consequently, according to concept of[36] the model expressions are expressed as follow:

$$\left(\frac{\partial \vec{u}}{\partial x}\right) + \left(\frac{\partial \vec{v}}{\partial y}\right) = 0, \tag{3}$$

$$\frac{\partial \vec{u}}{\partial t} + \vec{u}\left(\frac{\partial \vec{u}}{\partial x}\right) + \vec{v}\left(\frac{\partial \vec{u}}{\partial y}\right) = \upsilon_{\eta f}\left(\frac{\partial^2 \vec{u}}{\partial y^2}\right) - \frac{\nu_{nf}}{k^{\otimes}}(u) - F\left(u^2\right), \tag{4}$$

$$\frac{\partial T}{\partial t} + \vec{u}\left(\frac{\partial T}{\partial x}\right) + \vec{v}\left(\frac{\partial T}{\partial y}\right) = \alpha^{*}{}_{\eta f}\left(\frac{\partial^2 T}{\partial y^2}\right). \tag{5}$$

Here $(\vec{u}, \vec{v})$ signify the x and $y-$ directions components of velocity. Also $\upsilon_{\eta f}$ (Kinematic viscosity), $\beta_{\eta f}$ (Coefficient of thermal expansion), $\rho_{\eta f}$ (Density), $\alpha^{*}{}_{\eta f}$ (Thermal diffusivity) $\mu_{\eta f}$ (Viscosity), $(C_p)_{\eta f}$ (specific heat capacitance) of nanofluid respectively while ambient temperature is denoted by T.

A. Various model for water and CNTs

The above-mentioned factors are defined by Xue[12] as:

$$\frac{\mu_{\eta f}}{\mu_f} = (1-\phi)^{-2.5}, \quad \frac{\rho_{\eta f}}{\rho_f} = 1 - \phi + \phi\left[\frac{\rho_s}{\rho_f}\right],$$

$$\frac{(\rho\beta)_{\eta f}}{(\rho\beta)_f} = 1 - \phi + \phi\left[\frac{(\rho\beta)_s}{(\rho\beta)_f}\right], \quad \frac{\left(\rho C_p\right)_{\eta f}}{\left(\rho C_p\right)_f} = 1 - \phi + \phi\left[\frac{\left(\rho C_p\right)_s}{\left(\rho C_p\right)_f}\right],$$

$$\frac{\kappa_{\eta f}}{\kappa_f} = \left(\frac{1 - \phi + 2\phi\left(\frac{\kappa_s}{\kappa_s - \kappa_f}\right)\mathrm{In}\left(\frac{\kappa_s + \kappa_f}{2\kappa_f}\right)}{1 - \phi + 2\phi\left(\frac{\kappa_f}{\kappa_s - \kappa_f}\right)\mathrm{In}\left(\frac{\kappa_s + \kappa_f}{2\kappa_f}\right)}\right). \tag{6}$$

Here ϕ denotes the nanoparticles fraction to the base fluid. The subscript f and nf signifies the assets of base liquid and nanoparticles. Table I exhibits the numerical values of base fluids and nanoparticles.

TABLE I. Some numerical the thermo physical properties of SWCNTs and water.

Physical Properties		$c_p(kg^{-1}/k^{-1})$	$\rho\ (kg/m^3)$	$k(W/mk)$
Base fluid	Water	4197	997	0.613
Nanofluids	SWCNT	425	2600	6600

B. Subjected boundary constraints

Therefore, the boundary constraints related to the above-mentioned model problem is define[36] as:

$$\begin{aligned} &y = 0 \rightarrow \quad u = U_w, \quad v = 0, \quad T = T_s, \\ &y = h(t) \rightarrow \quad \frac{\partial u}{\partial y} = 0, \quad \frac{\partial T}{\partial y} = 0, \quad v = \frac{\partial T}{\partial y}. \end{aligned} \tag{7}$$

Here $h(t)$ represent the liquid film thickness.

C. Transformation factors

According to Schlichting and Gortler,[49] the boundary film width $\delta(x)$ is proportional to $(x\upsilon_f/U_w)^{\frac{1}{2}}$, and hence the factor η can be represented as:

$$\eta = y\sqrt{\frac{U_w}{x\upsilon_f}} = y\left(\frac{b}{(1-\alpha t)\upsilon_f}\right)^{\frac{1}{2}}. \tag{8}$$

According to the above mentioned explanation, we let $U(x) = U_w$ and define ξ, η and $\psi(x, y)$ as follows with new variables.[50]

$$\psi = \beta\sqrt{\left(\frac{\upsilon_f b}{1-\alpha t}\right)}x f(\eta), \tag{9}$$

$$T = T_0 - T_r(1-\alpha t)^{-\frac{3}{2}}\left[\frac{bx^2}{2\upsilon_f}\right]\theta(\eta), \tag{10}$$

$$\eta = \sqrt{\frac{b}{\upsilon_f(1-\alpha t)}}\left[\frac{y}{\beta}\right], \tag{11}$$

$$\vec{u} = \frac{\partial\psi}{\partial y} = \left(\frac{bx}{1-\alpha t}\right)f'(\eta), \tag{12}$$

$$\vec{v} = -\frac{\partial\psi}{\partial x} = -\beta\left[\sqrt{\frac{\upsilon_f b}{1-\alpha t}}\right]f(\eta). \tag{13}$$

So, the stream function $\psi(x, y)$ and $\beta > 0$ is the dimensionless form of liquid film thickness of fluid and define as

$$\beta = \left(hb/\upsilon_f\right)(1-\alpha t)^{-0.5}. \tag{14}$$

Introducing these variables in to the momentum and energy equations

$$\begin{aligned} &\frac{(1-\phi)^{-2.5}}{\left(1-\phi+\frac{\rho_s}{\rho_f}\phi\right)}f'''(\eta) + f(\eta)f''(\eta) - (f'(\eta))^2 - \frac{\lambda}{2}\left[\frac{\eta}{2}f''(\eta) + f'(\eta)\right] \\ &- \frac{1}{\left(1-\phi+\frac{\rho_s}{\rho_f}\phi\right)}\left[F(f'(\eta))^2 - f'(\eta)k\right] = 0 \end{aligned} \tag{15}$$

$$\frac{\left(\frac{1-\phi+2\phi\left(\frac{\kappa_s}{\kappa_s-\kappa_f}\right)\ln\left(\frac{\kappa_s+\kappa_f}{2\kappa_f}\right)}{1-\phi+2\phi\left(\frac{\kappa_f}{\kappa_s-\kappa_f}\right)\ln\left(\frac{\kappa_s+\kappa_f}{2\kappa_f}\right)}\right)}{\left(1-\phi+\frac{(\rho C_p)_s}{(\rho C_p)_f}\phi\right)P_r}\theta''(\eta)-2f'(\eta)\theta(\eta)+f(\eta)\theta'(\eta)$$
$$-\frac{\lambda}{2}[\eta\theta'(\eta)+3\theta(\eta)]=0. \tag{16}$$

Where the necessary boundary constraints takes the form

$$\begin{aligned}&\text{At } \eta=0\to f(0)=0,\quad f'(0)=1,\quad \theta(0)=1,\\&\text{At } \eta=1\to f(1)=\frac{\lambda}{2},\quad \theta'(1)=0.\end{aligned} \tag{17}$$

Here $P_r=\frac{\rho\upsilon_f C_p}{k_f}$ (Prandtl number), $\lambda=\frac{\alpha}{b}$ (unsteadiness parameter), $k=\frac{\upsilon_f}{K^{\circledast}\alpha}(1-at)$ (porous medium parameter), $F=\frac{C_b x}{\sqrt{K^{\circledast}}}$ (Darcy-porous medium parameter).

For the briefness, we write equations (15) and (16) as

$$f'''+A_1A_2\left\{ff''-(f')^2-\tfrac{\lambda}{2}\left[\tfrac{\eta}{2}f''+f'\right]\right\}-A_1\left(F(f')^2-kf'\right)=0, \tag{18}$$

$$\frac{A_3}{A_4P_r}\theta''-2f'\theta+f\theta'-\frac{\lambda}{2}[\eta\theta'+3\theta]=0. \tag{19}$$

Where A_1, A_2, A_3 and A_4 are constants and are defined as:

$$A_1=(1-\phi)^{2.5},\quad A_2=\left(1-\phi+\frac{\rho_s}{\rho_f}\phi\right),$$
$$A_3=\left(\frac{1-\phi+2\phi\left(\frac{\kappa_s}{\kappa_s-\kappa_f}\right)\ln\left(\frac{\kappa_s+\kappa_f}{2\kappa_f}\right)}{1-\phi+2\phi\left(\frac{\kappa_f}{\kappa_s-\kappa_f}\right)\ln\left(\frac{\kappa_s+\kappa_f}{2\kappa_f}\right)}\right),\quad A_4=\left(1-\phi+\frac{(\rho C_p)_s}{(\rho C_p)_f}\phi\right). \tag{20}$$

D. Final form of elementary features

For the present problem the physical quantities C_f (skin friction coefficient) and Nu (Nusselt number) are define as:

$$C_f=\frac{\tau_w}{\rho_f(U_w)^2},\quad Nu=\frac{q_w x}{k_f(T_r-T_0)}. \tag{21}$$

But the heat flux and skin friction at the surface are define in the following form

$$\tau_w=\mu_{nf}\left[\frac{\partial u}{\partial y}\right]_{y=0},\quad q_w=-k_{nf}\left[\frac{\partial T}{\partial y}\right]_{y=0}. \tag{22}$$

By inserting equation (22) into (21), we get the final non-dimensional form of C_f and Nu as:

$$C_f Re^{-0.5}=\frac{(1-\phi)^{-2.5}f''(0)}{\beta},\quad NuRe^{-0.5}=\frac{A_3\,\theta'(0)}{\beta}. \tag{23}$$

Where $Re=\frac{U_w}{\upsilon_f}$ (local Reynolds number).

III. SOLUTION BY HAM

HAM scheme is one of the substitute techniques and commonly applied to obtain the solution of nonlinear system of differential equations without linearization and discretization. First we calculate the primary estimates for the equations (18)–(19) as:

$$\hat{f}_0(\eta)=\eta-2\eta^2+\eta^3+3\delta\eta^2-2\delta\eta^3,\ \hat{\Theta}_0(\eta)=1-\eta. \tag{24}$$

The linear operators are selected as:

$$L_f(f)=\frac{\partial^3 f}{\partial\eta^3},\ L_\theta(\theta)=\frac{\partial^2\theta}{\partial\eta^2}. \tag{25}$$

The primary solution of the form:

$$L_f(\kappa_1+\kappa_2\eta+\kappa_3\eta^2)=0,\ L_\theta(\kappa_4+\kappa_5\eta)=0 \tag{26}$$

Here $\sum_{j=1}^{5}\kappa_j$, where $j=1,2,3,4,5$ are arbitrary constants.

Zero order deform to the following form with boundary conditions is

$$(1-\chi)L_f\left[\hat{f}(\eta,\chi)-f_0(\eta)\right]=\chi h_f N_f\left[\hat{f}(\eta,\chi)\right], \tag{27}$$

$$(1-\chi)L_\theta\left[\hat{\theta}(\eta,\chi)-\theta_0(\eta)\right]=\chi h_\theta N_\theta\left[\hat{f}(\eta,\chi),\hat{\theta}(\eta,\chi)\right], \tag{28}$$

$$\begin{aligned}&\hat{f}(\eta,\chi)\Big|_{\chi=0}=0,\quad \frac{\hat{f}(\eta,\chi)}{d\eta}\Big|_{\chi=0}=1,\quad \hat{\theta}(\eta,\chi)\Big|_{\chi=0}=1,\\&\hat{f}(\eta,\chi)\Big|_{\chi=1}=\frac{\lambda}{2},\quad \frac{\hat{\theta}(\eta,\chi)}{d\eta}\Big|_{\chi=1}=0,\end{aligned} \tag{29}$$

The considerable nonlinear operators N_f, N_θ are intended as

$$N_f\left[\hat{f}(\eta;\chi)\right]=\hat{f}_{\eta\eta\eta}(\eta;\chi)+\hat{f}_\eta(\eta;\chi)\hat{f}(\eta;\chi)-A_1A_2(1-A_1F)\hat{f}_{\eta\eta}(\eta;\chi)$$
$$-A_1k\hat{f}_\eta(\eta;\chi)-A_1A_2\frac{\lambda}{2}\left(\frac{\eta}{2}\hat{f}_{\eta\eta}(\eta;\chi)-\hat{f}_\eta(\eta;\chi)\right), \tag{30}$$

$$N_\theta\left[\hat{\theta}(\eta;\chi),\hat{f}(\eta;\chi)\right]=\frac{A_3}{A_4\,Pr}\hat{\theta}_{\eta\eta}(\eta;\chi)-2\hat{f}_\eta(\eta;\chi)\hat{\theta}(\eta;\chi)$$
$$+\hat{f}(\eta;\chi)\hat{\theta}_\eta(\eta;\chi)-\left(\eta\frac{\lambda}{2}\hat{\theta}_\eta(\eta;\chi)+3\hat{\theta}(\eta;\chi)\right). \tag{31}$$

When χ shifted from 0 to 1, then evaluating with the given boundary constraints

$$\hat{f}(\eta;0)=\hat{f}(\eta),\hat{\theta}(\eta;0)=\hat{\theta}(\eta), \tag{32}$$

$$f_m(\eta)=\frac{1}{m!}\hat{f}_\eta(\eta,\chi)\Big|_{\chi=0},\theta_m(\eta)=\frac{1}{m!}\hat{\theta}_\eta(\eta,\chi)\Big|_{\chi=0}. \tag{33}$$

At $\chi = 1$, we get:

$$f(\eta) = f_0(\eta) + \sum_{m=1}^{\infty} f_m(\eta), \quad \theta(\eta) = \theta_0(\eta) + \sum_{m=1}^{\infty} \theta_m(\eta). \tag{34}$$

Now differentiate 0^{th} order expression, the deformation equations i^{th} order with boundary conditions reduced as

$$\begin{aligned} &L_f\{f_m(\eta) - \xi_m f_{m-1}(\eta)\} = h_f R_m^f(\eta), \\ &L_\theta\{\theta_m(\eta) - \xi_m \theta_{m-1}(\eta)\} = \hbar_\theta R_m^\theta(\eta). \end{aligned} \tag{35}$$

$$\begin{aligned} &f_i = 0, f_i' = 1, \theta_i = 1 \quad at \quad \eta = 0, \\ &\hat{f}_i = \frac{\lambda}{2}, \theta_i' = 0 \quad at \quad \eta = 1. \end{aligned} \tag{36}$$

$$\begin{aligned} R_m^f(\eta) = f_{m-1}^{iii} + \sum_{j=0}^{m-1} f_{m-1-j}' f_k - A_1 A_2 (1 - A_1 F) \sum_{j=0}^{m-1} f_{m-1-j}'' \\ - A_1 k \sum_{j=0}^{m-1} f_{m-1-j}' - A_1 A_2 \frac{\lambda}{2}\left(\frac{\eta}{2} \sum_{j=0}^{m-1} f_{m-1-j}'' - \sum_{j=0}^{m-1} f_{m-1-j}'\right), \end{aligned} \tag{37}$$

$$\begin{aligned} R_m^\theta(\eta) = \frac{A_3}{A_4 \Pr} \theta_{m-1}'' - 2 \sum_{j=0}^{m-1} f_{m-1-j}' \theta_k + \sum_{j=0}^{m-1} \theta_{m-1-j}' f_k \\ - \left(\eta \frac{\lambda}{2} \sum_{j=0}^{m-1} \theta_{m-1}' + 3 \sum_{j=0}^{m-1} \theta_{m-1}\right). \end{aligned} \tag{38}$$

Where

$$\chi_m = \begin{cases} 1, & m > 1 \\ 0, & m \le 1 \end{cases}. \tag{39}$$

IV. GRAPHS AND DISCUSSION

The results of Equations (18)–(19) through boundary constraint (17) are established by employing HAM scheme. Figure 1 show the physical sketch of the flow phenomena. Figure 2 presents the comparison of HAM and numerical scheme (NDSolve) results for SWCNTs and a tremendous settlement is established between both sachems. Furthermore, impacts of various model factors like P_r (Prandtl number), λ (unsteadiness factor), k (porous medium factor), F (Darcy-porous medium factor) on $f'(\eta)$ (velocity profile), $\theta(\eta)$ (temperature profile), C_f (coefficients of skin friction) and Nu (Nusselt number) versus SWCNTs-water nanoparticles are explained through Figures 3–8. The fixed values of these assorted factors utilized in Figures are ($\lambda = 0.3$, $\phi = 0.1$, F = 0.2, M = 0.5, Pr = 6.5). Figure 3 reports the variation in $f'(\eta)$ by means of λ (unsteady parameter) of SWCNTs-water thin nano-liquid. It is worth stating here that $\lambda = 0$ designate the steady case and $\lambda \neq 0$ declare the unsteady condition. From the graphical inspection $f(\eta)$ is prominent the enhancing function of λ. Therefore, intensification in the magnitude of λ yield to decline the width of the film, suddenly, the inner velocity of finite film improves the outward velocity of liquid. This causes an improvement in λ upsurges the stretchable velocity. Generally, the velocity of thin film in steady case is quicker than the velocity unsteady

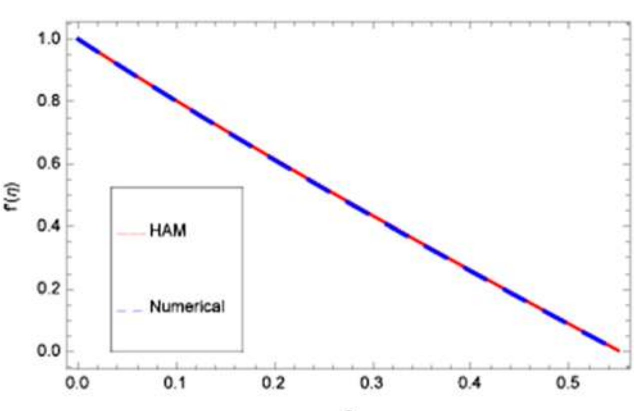

FIG. 2. Numerical comparison for velocity.

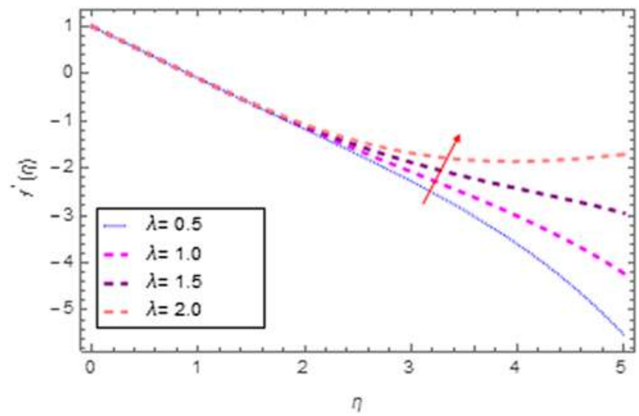

FIG. 3. $f'(\eta)$ (velocity profile) for four different values of λ (unsteadiness factor) for SWCNT-water.

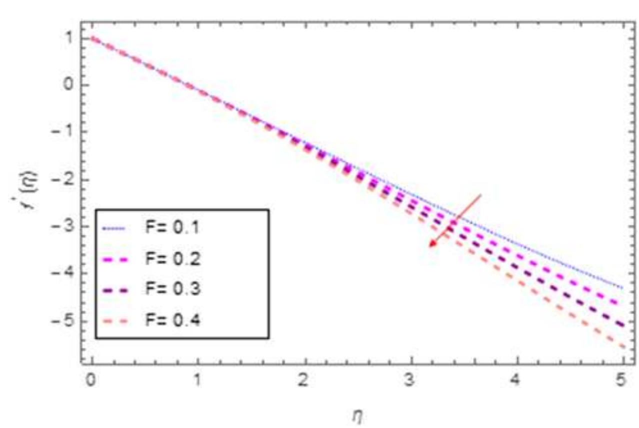

FIG. 4. $f'(\eta)$ (velocity profile) for four different values of F (Darcy porous medium factor) for SWCNT-water.

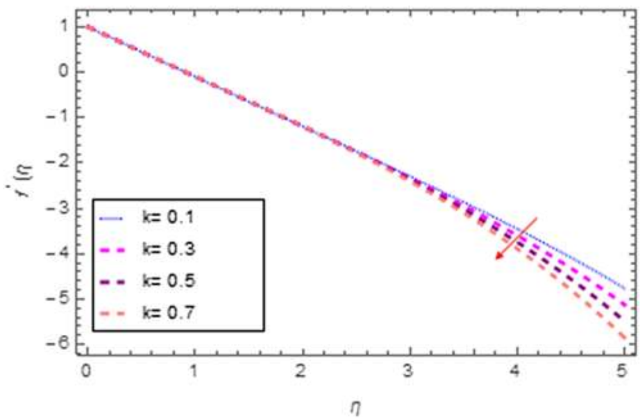

FIG. 5. $f'(\eta)$ (velocity profile) for four different values of k (Porous medium factor) for SWCNT-water.

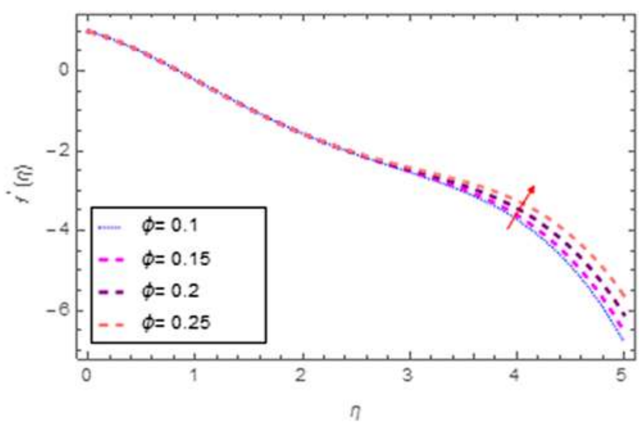

FIG. 6. $f'(\eta)$ (velocity profile) for four different values of ϕ (volume fraction of nanofluid) for SWCNT-water.

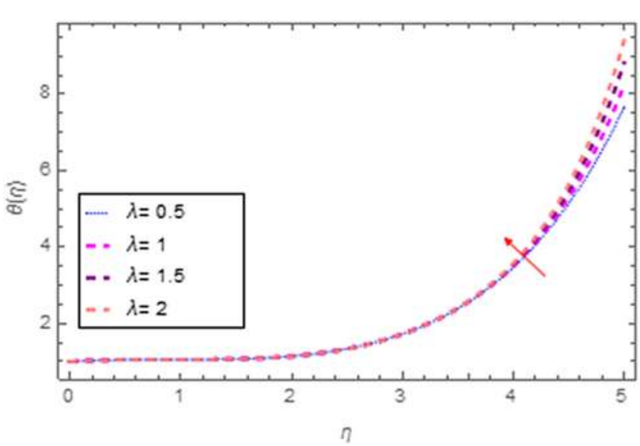

FIG. 7. $\theta(\eta)$ (Temperature profile) for four different values of λ (Steadiness factor) for SWCNT-water.

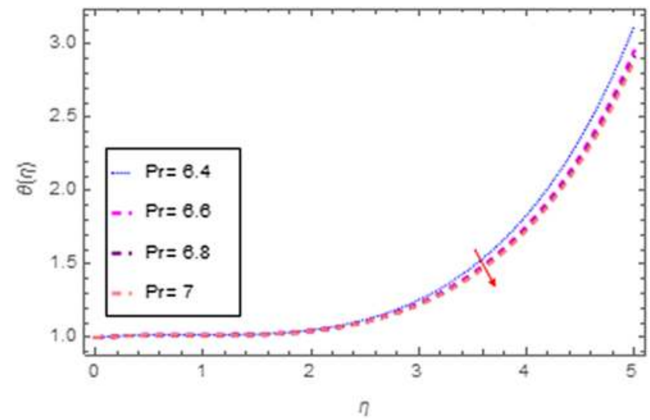

FIG. 8. $\theta(\eta)$ (Temperature profile) for four different values of Pr (Prandtl number) for SWCNT-water.

state. Figure 4 address the variations F viva $f'(\eta)$. Here, it is noted that F is the decaying function of $f'(\eta)$ for SWCNTs-water nanoparticles. In fact, a raise in F produce resilience in thin liquid film which yield to decline $f'(\eta)$. Physically, by increasing the magnitude of F, the inside thin film nanofluid velocity is declined, however there is no impact of F on nanofilm film thickness. In state of permeable openings with greater openings dimension, and porous surface expended through liquid-solid interface, which upsurges the viscous interference. Therefore, an improvement in F produce a well flow opposition, so velocity of fluid is declined. Figure 5 highlights the $f'(\eta)$ variation for k (porous medium factor) for thin film SWCNTs-water nanoliquid. Obviously, from the sketch, we noted that when the magnitude of k rises then the velocity $f'(\eta)$ profile is also incremented. Physically, by enhancing the magnitude of k, a fall in the spongy region permeability is produced. Consequently, minor opening is available for thin nanofluid to move and hence, we observe that thin nanoliquid velocity is declined. Figure 6 portrays the impression of ϕ (volume fraction of nanoparticles) on $f'(\eta)$ (Velocity profiles) for thin film water based nanofluid with SWCNTs. It is perceived that for SWCNTs-water nanoparticles, as the magnitude of ϕ enhances, the $f'(\eta)$ of the thin nano-fluid improve. Physically, the basic fact is that by injecting greater quantities of nanoparticles ϕ in case of thin nano-liquid; improves the heat transport and cohesive forces between the liquid particles and these particles become fragile to stop the quicker fluid movement. Therefore, the heat transport in tinny sort of particles is faster than the dense ingredients. Figure 7 is shown to investigate the communication between the λ (porosity factor) and the $\theta(\eta)$ of thin film SWCNTs nanoliquid. The $\theta(\eta)$ profile and the thermal film thickness enhance as the magnitude of λ upsurges. It is perceived form the sketch that in the existence of permeable media generates an enhancement in the opposition against the thin nanofluid movement which ultimately leads to a stronger $\theta(\eta)$ profile. Figure 8 displays the significance of the Pr (Prandtl number) on the $\theta(\eta)$ profile thin film SWCNTs nanoparticle. Enhancements in Pr rapidly fall $\theta(\eta)$ as well as decline the thermal boundary film thickness

TABLE II. k_{nf} (Thermal conductivity) of SWCNTs with different values of ϕ.

Volume Fraction ϕ	k_{nf} for SWCNTs
0	0.243
0.1	0.271
0.2	0.300
0.3	0.335
0.4	0.367

TABLE III. Comparing the HAM and Numerical results of velocity using SWCNTs nanoliquid.

η	HAM Solution	Numerical solution	Error
0.0	1.00	1.00	0.00000
0.1	0.802776	0.801295	1.4×10^{-3}
0.2	0.615071	0.612715	2.3×10^{-3}
0.3	0.434626	0.431988	2.6×10^{-3}
0.4	0.259548	0.257175	2.3×10^{-3}
0.5	0.088273	0.086636	1.6×10^{-3}

of nanofluid. Due to increase the magnitude of Pr, the viscosity of SWCNTs water based nanofluid also increases as a result in lessening in $\theta(\eta)$ profile produced.

In Table II different values of k_{nf} (Thermal conductivity) are calculated of SWCNTs using numerous magnitude of ϕ. In Table III the HAM and numerical (ND-Solve scheme) results are compared for velocity of SWCNTs nanofluid and a tremendous settlement is established between both sachems. Table IV exhibits the mathematical values of HAM solutions for $f''(0)$ and $\Theta'(0)$ up to 10^{th} order estimation using several value of physical factors for SWCNTs nanoliquid. Clearly, from Table IV perceived that HAM technique is a rapidly convergent. Table V displays the influence of some physical quantities

TABLE IV. The convergence table of HAM for SWCNTs up to 10^{th} order of approximations for $f''(0)$ and $\Theta'(0)$.

N0. Of iteration	$f''(0)$	$\Theta'(0)$
2	2.03928	0.116475
4	2.05164	0.125325
6	2.05241	0.125934
8	2.05246	0.125986
9	2.05247	0.125994
10	2.05247	0.125994

TABLE V. Reveals the Numerical values for $-f''(0)$and $-\Theta'(0)$ for SWCNTs.

ϕ	λ	F	$-f''(0)$	$-\Theta'(0)$
0.1	0.3	0.4	2.0557	0.128473
0.2			2.03731	0.125752
0.3			2.20581	2.20581
0.1	0.3		2.0557	0.128473
	0.4		2.0448	0.12712
	0.5		2.05239	0.128493
	0.3	0.4	2.0557	0.128473
		0.5	2.0502	0.126082
		0.6	2.06311	0.126411

(ϕ, F, λ) on $-f''(0)$ and $-\theta'(0)$ for SWCNTs. Through Table V, it is noted that an enhancement in (ϕ, F) leads to improve $-f''(0)$ while (λ) show the opposite behavior. Similarly, in same table the rising values of (ϕ, λ) leads to enhance $-\theta'(0)$ while (F) presents reverse behavior.

V. CONCLUSIONS

In present work, the HAM technique is employed to get the solution of Darcy Forchheimer two dimensional thin liquid stream of SWCNT-water nanoliquid and associated heat transport problem over a unsteady stretching plate. The accuracy of HAM technique is tested with the numerical scheme mathematically and graphically. The judgment specifies that HAM technique has an excellent compatibility with the numerical facts. Afterwards, the confirming models, the effect of various physical factors like ϕ, λ, k, F, Pr on the temperature and velocity significance have been examined in details. Present analysis attempts to the following remakes.

- The larger values of k and F yield reduction in thin liquid $f'(\eta)$.
- It is perceived that the components of $f'(\eta)$ and $\theta(\eta)$ are directly related to λ. An increment in $f'(\eta)$ and $\theta(\eta)$ is seem with the intensification in λ.
- An intensification in ϕ leads to improve $f'(\eta)$.
- There is a reduction in $\theta(\eta)$ for high value of Pr.
- $-f''(0)$ via ϕ, F enhances, but λ shows opposite behavior.
- Nu (heat exchange rate) via ϕ, λ augments, while F displays reverse trend.
- An excellent agreement is found for the convergence of HAM and numerical method.

REFERENCES

[1] S. K. Das, S. U. S. Choi, and H. E. Patel, "Heat transfer in nanofluids–A review," Heat Transfer Eng. **27**, 3–19 (2006).
[2] W. Yu, D. M. France, S. U. Choi, and J. L. Routbort, "Review and assessment of nanofluid technology for transportation and other applications," Argonne National Laboratory (ANL), 2007.
[3] G. L. Mellor, P. J. Chapple, and V. K. Stokes, "On the flow between a rotating and a stationary disk," J. Fluid Mech. **31**, 95–112 (1968).
[4] B. J. Gireesha, B. Mahanthesh, and K. L. Krupalakshmi, "Hall effect on two-phase radiated flow of magneto-dusty-nanoliquid with irregular heat generation/consumption," Results in Physics **7**, 4340–4348 (2017).
[5] B. Mahanthesh, B. J. Gireesha, G. T. Thammanna, S. A. Shehzad, F. M. Abbasi, and R. S. R. Gorla, "Nonlinear convection in nano Maxwell fluid with nonlinear thermal radiation: A three-dimensional study," Alexandria Engineering Journal **57**, 1927–1935 (2018).
[6] P. B. Sampath Kumar, B. Mahanthesh, B. J. Gireesha, and S. A. Shehzad, "Quadratic convective flow of radiated nano-Jeffrey liquid subject to multiple convective conditions and Cattaneo-Christov double diffusion," Applied Mathematics and Mechanics **39**, 1311–1326 (2018).
[7] B. Mahanthesh, B. J. Gireesha, S. A. Shehzad, A. Rauf, and P. B. Sampath Kumar, "Nonlinear radiated MHD flow of nanoliquids due to a rotating disk with irregular heat source and heat flux condition," Physica B: Condensed Matter **537**, 98–104 (2018).
[8] A. Sahu and B. Mahanthesh, "Exact solutions for unsteady mixed convection flow of nanoliquid with exponential heat source: Bruggeman and Batchelor nanofluid model," Journal of Nanofluids **7**, 1164–1171 (2018).
[9] T. S. Ashlin and B. Mahanthesh, "Exact solution of non-coaxial rotating and non-linear convective flow of $Cu–Al_2O_3–H_2O$ hybrid nanofluids over

an infinite vertical plate subjected to heat source and radiative heat," J. Nanofluids **8**, 781–794 (2019).
[10] S. U. S. Choi and J. A. Eastman, "Enhancing thermal conductivity of fluids with nanoparticles," The Proceedings of the 1995 ASME International Mechanical Engineering Congress and Exposition, San Francisco, USA, ASME, FED 231/MD 66 (1995), 99–105.
[11] S. Iijima, "Helical microtubules of graphitic carbon," Nature **354**, 56–58 (1991).
[12] Q. Xue, "Model for thermal conductivity of carbon nanotube-based composites," Phys. B Condens. Matter **368**, 302–307 (2005).
[13] Y. Ding, H. Alias, D. Wen, and R. A. Williams, "Heat transfer of aqueous suspensions of carbon nanotubes (CNT nanofluids)," Int. J. Heat Mass Transfer **49**, 240–250 (2006).
[14] M. Imtiaz, T. Hayat, A. Alsaedi, and B. Ahmad, "Convective flow of carbon nanotubes between rotating stretchable disks with thermal radiation effects," Int. J. Heat Mass Transfer **101**, 948–957 (2016).
[15] T. Hayat, F. Haider, T. Muhammad, and A. Alsaedi, "On Darcy-Forchheimer flow of carbon nanotubes due to a rotating disk," Int. J. Heat Mass Transfer **112**, 248–254 (2017).
[16] B. Mahanthesh, B. J. Gireesha, N. S. Shashikumar, and S. A. Shehzad, "Marangoni convective MHD flow of SWCNT and MWCNT nanoliquids due to a disk with solar radiation and irregular heat source," Physica E **94**, 25–30 (2017).
[17] S. Nasir, S. Islam, T. Gul, Z. Shah, M. A. Khan, W. Khan, A. Z. Khan, and S. Khan, "Three-dimensional rotating flow of MHD single wall carbon nanotubes over a stretching sheet in presence of thermal radiation," Applied Nanoscience **8**, 1361–1378 (2018).
[18] O. Reynolds, "On the theory of lubrication and its application to Mr. Beauchamp tower's experiments, including an experimental determination of the viscosity of olive oil," Philosophical Transactions of Royal Society of London **177**, 191–203 (1886).
[19] A. Oron, S. H. Davis, and S. G. Bankoff, "Long-scale evolution of thin liquid films," Reviews of Modern Physics **69**, 931–980 (1997).
[20] U. Thiele, B. Goyeau, and M. G. Velarde, "Stability analysis of thin film flow along a heated porous wall," Physics of Fluids **21** (2009).
[21] A. M. Siddiqui, H. Ashraf, A. Walait, and T. Haroon, "On study of horizontal thin film flow of Sisko fluid due to surface tension gradient," Applied Mathematics and Mechanics **36**, 847–862 (2015), (English Edition).
[22] G. M. Prashant, T. Jagdish, and M. S. Abel, "Thin film flow and heat transfer on an unsteady stretching sheet with thermal radiation internal heating in presence of external magnetic field," Physics Flu-Dyn. **3**, 1–16 (2016).
[23] N. S. Khan, T. Gul, S. Islam, and W. Khan, "Thermophoresis and thermal radiation with heat and mass transfer in a magneto-hydrodynamic thin film second-grade fluid of variable properties past a stretching sheet," Eur. Phys. J. Plus **132**, 1–20 (2017).
[24] T. Gul, S. Nasir, S. Islam, Z. Shah, and M. A. Khan, "Effective Prandtl number model influences on the γAl_2O_3–H_2O and γAl_2O_3–$C_2H_6O_2$ nanofluids spray along a stretching cylinder," Arabian Journal for Science and Engineering 1–18 (2018).
[25] Z. Shah, E. Bonyah, S. Islam, W. Khan, and M. Ishaq, "Radiative MHD thin film flow of Williamson fluid over an unsteady permeable stretching," Heliyon **4**, e00825 (2018).
[26] M. Jawad, Z. Shah, S. Islam, E. Bonyah, and A. A. Khan, "Darcy-Forchheimer flow of MHD nanofluid thin film flow with Joule dissipation and Navier's partial slip," J. Phys. Commun. (2018).
[27] N. Khan, S. Zuhra, Z. Shah, E. Bonyah, W. Khan, and S. Islam, "Slip flow of Eyring-Powell nanoliquid film containing graphene nanoparticles," AIP Adv. **8**, 115302 (2018).
[28] Z. Khan, R. A. Shah, S. Islam, H. Jan, B. Jan, and H. Rasheed, "MHD flow and heat transfer analysis in the wirecoating process using elastic-viscous," Coatings **7**, 15 (2017).
[29] S. Naghdi, K. Y. Rhee, D. Hui, and S. J. Paark, "A review of conductive metal nanomaterials as conductive, transparent, and flexible coatings, thin films, and conductive fillers: Different deposition methods and applications," Coatings **8**, 278 (2018).
[30] L. J. Crane, "Flow past a stretching plate," Zeitschrift für Angewandte Mathematik und Physic ZAMP **21**, 645–647 (1970).
[31] C. Y. Wang, "Liquid film on an unsteady stretching surface," Quart. Appl. Math. **48**, 601–610 (1990).
[32] B. J. Gireesha, R. S. R. Gorla, and B. Mahanthesh, "Effect of suspended nanoparticles on three-dimensional MHD flow, heat and mass transfer of radiating Eyring-Powell fluid over a stretching sheet," Journal of Nanofluids **4**(4), 474–484 (2015).
[33] B. Mahanthesh, B. J. Gireesha, S. Manjunatha, and R. S. R. Gorla, "Effect of viscous dissipation and Joule heating on three-dimensional mixed convection flow of nano fluid over a non-linear stretching sheet in presence of solar radiation," J. Nanofluids **6**, 735–742 (2017).
[34] B. Mahanthesh, B. J. Gireesha, B. C. P. Kumara, and N. S. Shashikumar, "Marangoni convection radiative flow of dusty nanoliquid with exponential space dependent heat source," Nuclear Engineering and Technology **49**, 1660–1668 (2017).
[35] B. J. Gireesha, B. Mahanthesh, G. T. Thammanna, and P. B. Sampathkumar, "Hall effects on dusty nanofluid two-phase transient flow past a stretching sheet using KVL model," Journal of Molecular Liquids **256**, 139–147 (2018).
[36] B. Mahanthesh and B. J. Gireesha, "Dual solutions for unsteady stagnation-point flow of Prandtl nanofluid past a stretching/shrinking plate," Defect and Diffusion Forum **388**, 124–134 (2018).
[37] M. Fakour, A. Rahbari, E. Khodabandeh, and D. D. Ganji, "Nanofluid thin film flow and heat transfer over an unsteady stretching elastic sheet by LSM," Journal of Mechanical Science and Technology **32**, 177–183 (2018).
[38] P. Forchheimer, "Wasserbewegung durch boden," Zeitschrift Ver D Ing, **45**, 1782–1788 (1901).
[39] M. Muskat, *The flow of homogeneous fluids through porous media* (Edwards, MI, 1946).
[40] P. Cheng and W. Minkowycz, "Free convection about a vertical flat plate embedded in a porous medium with application to heat transfer from a dike," Journal of Geophysical Research **82**, 2040–2044, https://doi.org/10.1029/jb082i014p02040 (1977).
[41] J. Merkin, "Free convection boundary layers on axi-symmetric and two-dimensional bodies of arbitrary shape in a saturated porous medium," International Journal of Heat and Mass Transfer **22**, 1461–1462 (1979).
[42] A. Nakayama and H. Koyama, "Free convective heat transfer over a non-isothermal body of arbitrary shape embedded in a fluid-saturated porous medium," Journal of Heat Transfer **109**, 125–130 (1987).
[43] B. J. Gireesha, P. B. Kumar, Sampath, B. Mahanthesh, S. A. Shehzad, and F. M. Abbasi, "Nonlinear gravitational and radiation aspects in nanoliquid with exponential space dependent heat source and variable viscosity," Microgravity Science and Technology **30**, 257–264 (2018).
[44] Z. Shah, A. Dawar, S. Islam, I. Khan, D. I. C. Ching, and A. Khan "Cattaneo-Christov model for electrical magnetite micropoler Casson ferrofluid over a stretching/shrinking sheet using effective thermal conductivity model," Case Stud. Therm. Eng. (2018).
[45] Z. Shah, A. Dawar, S. Islam, I. Khan, and D. L. C. Ching, "Darcy-Forchheimer flow of radiative carbon nanotubes with microstructure and inertial characteristics in the rotating frame," Case Stud. Therm. Eng. (2018).
[46] T. Muhammad, A. Alsaedi, S. A. Shehzad, and T. Hayat, "A revised model for Darcy-Forchheimer flow of Maxwell nanofluid subject to convective boundary condition," Chin J Phys **55**, 963–976 (2017).
[47] A. K. Alzahrani, "Importance of Darcy–Forchheimer porous medium in 3D convective flow of carbon nanotubes," Physics Letters A **384**, 2938–2943 (2018).
[48] A. Khan, Z. Shah, S. Islam, S. Khan, W. Khan, and Z. A. Khan, "Darcy–Forchheimer flow of micropolar nanofluid between two plates in the rotating frame with non-uniform heat generation/absorption," Adv. Mech. Eng. **10**, 1–16 (2018).
[49] S. J. Liao, "An optimal homotopy-analysis approach for strongly nonlinear differential equations," Commun. Nonlinear Sci. Numer. Simul. **15**, 2003–2016 (2010).
[50] Z. Shah, S. Islam, H. Ayaz, and S. Khan, "Radiative heat and mass transfer analysis of micropolar nanofluid flow of Casson fluid between two rotating

parallel plates with effects of Hall current," ASME Journal of Heat Transfer **141**, 022401-1 (2019).
[51] Z. Shah, S. Islam, T. Gul, E. Bonyah, and M. Altaf Khan, "The electrical MHD and hall current impact on micropolar nanofluid flow between rotating parallel plates," Results Phys. **9**, 1201–1214 (2018).
[52] U. Asad, O. A. Ebraheem, Z. Shah, M. Ayaz, and S. Islam, "Nanofluids thin film flow of Reiner-Philippoff fluid over an unstable stretching surface with Brownian motion and thermophoresis effects," Coatings **9**, 21 (2019).
[53] Z. Palwasha, N. Khan, Z. Shah, I. Islam, and E. Bonyah, "Study of two-dimensional boundary layer thin film fluid flow with variable thermophysical properties in three dimensions space," AIP Advances **8**, 105318 (2018).
[54] S. Zuhra, N. Khan, Z. Shah, I. Islam, and E. Bonyah, "Simulation of bioconvection in the suspension of second grade nanofluid containing nanoparticles and gyrotactic microorganisms," AIP Advances **8**, 105210 (2018).
[55] A. Ali, M. Sulaiman, S. Islam, Z. Shah, and E. Bonyah, "Three-dimensional magnetohydrodynamic (MHD) flow of Maxwell nanofluid containing gyrotactic micro-organisms with heat source/sink," AIP Advances **8**, 085303 (2018).